Research Square

Preprints are preliminary reports that have not undergone peer review.
They should not be considered conclusive, used to inform clinical practice,
or referenced by the media as validated information.

A Regional Climate Modeling Investigation of Wetland-Related Coupled Hydrologic–Atmospheric Processes in Central South America

Anthony Schrapffer

anthony.schrapffer@edhec.edu

EDHEC Business School https://orcid.org/0000-0003-0177-5505

Jan Polcher

Laboratoire de Météorologie Dynamique: Laboratoire de Meteorologie Dynamique

Anna Sörensson

CIMA: Centro de Investigaciones del Mar y la Atmosfera

Lluis Fita Borrell

CIMA: Centro de Investigaciones del Mar y la Atmosfera

Claudio Menéndez

CIMA: Centro de Investigaciones del Mar y la Atmosfera

Research Article

Keywords: Pantanal, Land–Atmosphere Interactions, Regional Climate Modeling, Wetlands

Posted Date: March 9th, 2026

DOI: https://doi.org/10.21203/rs.3.rs-8688042/v1

License: This work is licensed under a Creative Commons Attribution 4.0 International License.
Read Full License

A Regional Climate Modeling Investigation of Wetland-Related Coupled Hydrologic–Atmospheric Processes in Central South America

Anthony Schrapffer[1,3,4,5], Jan Polcher[2], Anna Sörensson[3,4,5], Lluis Fita Borrell[3,4,5], Claudio Menéndez[3,4,5]

[1]EDHEC Climate Institute, Paris, France.
[2]Laboratoire de Météorologie Dynamique (LMD), IPSL, CNRS, École Polytechnique, Palaiseau, France.
[3]UBA - CONICET, Centro de Investigaciones del Mar y la Atmósfera (CIMA), Buenos Aires, Argentina.
[4]CNRS – IRD – CONICET – UBA, Institut Franco-Argentin d'Études sur le Climat et ses Impacts (IRL IFAECI), Buenos Aires, Argentina.
[5]Departamento de Ciencias de la Atmósfera y los Océanos, UBA, FCEN, Buenos Aires, Argentina.

Contributing authors: anthony.schrapffer@edhec.edu;

Abstract

This study investigates how the Pantanal, one of the world's largest tropical floodplains, modulates local and regional climate in central South America through coupled land–atmosphere processes. Using the RegIPSL regional climate modeling framework, two simulations covering the 1998–2019 period were conducted: one including an explicit floodplain scheme and one without it. The floodplain-enabled simulation exhibits a substantially improved representation of the hydrological cycle over the Pantanal and Upper Paraguay River Basin, particularly through enhanced evapotranspiration, increased moisture recycling, and more realistic river discharge. Results show that activating the floodplain scheme increases precipitation across most of the Pantanal and surrounding regions, primarily by raising the number of rainy days during the wet season. However, convection is suppressed over the most heavily flooded areas, consistent with wetland-breeze dynamics and stabilized boundary-layer conditions. At regional scales, enhanced evapotranspiration transforms the Pantanal into an atmospheric moisture source, increasing lower-tropospheric humidity, moist static energy, and convective potential downstream. The altered surface fluxes

weaken the Chaco Low and modify the South American Low-Level Jet, reducing large scale atmospheric moisture transport over the Pantanal but strengthening it along the eastern Andes, ultimately increasing precipitation in parts of northern Argentina. These findings highlight the crucial role of tropical floodplains in shaping regional climate and underscore the importance of representing wetland processes in Earth system and regional climate models.

Keywords: Pantanal, Land–Atmosphere Interactions, Regional Climate Modeling, Wetlands

1 Introduction

The ground surface conditions affect the climate and, as there can be significant feedbacks between soil moisture and the atmosphere (Dirmeyer 2011; Seneviratne et al. 2013), these feedbacks can be more pronounced in large tropical floodplains, as they are subject to higher available energy, which enhances the contrast between flooded areas and adjacent dry regions. The present work aims to understand how large tropical floodplains, such as the Pantanal in South America, can influence local and regional climate using a land-atmosphere coupled climate model and the representation of floodplains in the Land Surface Model (LSM).

Land surface features with strong horizontal gradients, such as variations in soil moisture, flooded areas, and open water surfaces, have been extensively studied for their impact on land-atmosphere interactions. Several studies have investigated the influence of the Great Lakes on precipitation, particularly snowfall (Gula and Richard Peltier 2012; Notaro et al. 2015; Wright et al. 2013; Lucas-Picher et al. 2017), and the coupling dynamics of tropical lakes such as Lake Victoria (Finney et al. 2019). Wetlands such as the Niger Inland Delta floodplains were to influence rainfall and Mesoscale Convective Systems (MCS) formation such as in Taylor (2010), with further investigations extending to sub-Saharan African wetlands (Taylor et al. 2018). High concentration of irrigated land in tropical regions sensitive to land-atmosphere interactions, such as the Ganges basins, may also be affected in a similar way (Harding et al. 2013). At a global scale, Vanderkelen et al. (2021) examined the atmospheric impacts of open water reservoirs through global coupled simulations. This study has only shown local impact over the largest reservoirs reservoirs with a reduction of surface temperature and of temperature extremes.

The presence of floodplains and their related enhanced evapotranspirative fluxes can affect the vertical profile of the Planetary Boundary Layer (PBL; Bonan 1995; Koster et al. 2004; Krinner 2003). These changes, driven by increased atmospheric moisture and heat content (indicated by higher equivalent potential temperature) and Convective Available Potential Energy (CAPE; Kohler et al. 2010; Adler et al. 2011), may further influence regional air mass advection (Kumar et al. 2020; Koster et al. 2016; Schubert et al. 2008). This might be amplified in tropical floodplains in drier regions, such as Savannahs: because (1) evapotranspirative fluxes will be higher over the flooded areas compared to the surrounding, and (2) temperature and heat fluxes

horizontal gradient discontinuities will be stronger at the surface compared to wetter / colder regions.

In the literature, two main processes have been identified to be relevant for the Pantanal: one related to the local contrast between wet and dry surfaces and another involving the larger scale impact of local wetter surfaces.

Previous studies show that wetlands strongly modulate local convection through surface–atmosphere interactions. Using observations over African floodplains, Taylor (2010) found that Mesoscale Convective Systems (MCSs) preferentially initiate or re-intensify over the drier areas surrounding flooded wetlands, particularly during the afternoon and evening. This result was confirmed by Taylor et al. (2018) using satellite estimates of wetland extent, rainfall, and cloud cover, which showed enhanced convection at wetland margins but suppressed convection over flooded surfaces.

Taylor (2010) shows that MCSs are more likely to trigger / re-intensify in the dryer area surrounding the flooded wetlands because of the extra moisture source, and this occurs principally during the afternoon / evening. This result was confirmed by Taylor et al. (2018) using satellite estimates of wetland extent, rainfall, and cloud cover, which showed enhanced convection at wetland margins but suppressed convection over flooded area.

This pattern is driven by differential surface heating between cool, moist wetlands and warmer, drier surrounding land. During peak daytime heating, the surrounding land warms more rapidly, creating horizontal temperature and pressure gradients. These gradients induce a low-level flow from the wetland toward the warmer land, producing divergence over the wetland and convergence near its edges. Over flooded areas, reduced sensible heat flux and enhanced latent cooling stabilize the boundary layer, suppressing vertical motion and inhibiting convection. This phenomenon is similar a "wetland breeze," analogous to the river-breeze mechanism that suppresses precipitation over large Amazonian rivers (Silva Dias et al. 2004; Paiva et al. 2011). Therefore, wetlands can influence local precipitation and modify regional circulation, which in turn can affect regional rainfall, particularly in regions such as the Sahel where precipitation is dominated by long-lived MCS.

The precipitation response described by Taylor (2010) and Taylor et al. (2018) can be partly explained by contrasts in Bowen ratio (H/LE) between wet floodplains and surrounding dry soils. This mechanism was explored by Adler et al. (2011), who examined the atmospheric response to a wet soil band anomaly over West Africa. In weak-advection conditions, wet soils increase boundary-layer equivalent potential temperature (θ_e), enhancing Convective Available Potential Energy (CAPE), but simultaneously lower the actual temperature, increasing Convective Inhibition (CIN). Although CAPE is higher over wet surfaces, the increased CIN suppresses convection by limiting upward motion over the moist band. Low-level horizontal advection from wet to dry areas transports high-θ_e air into the surrounding regions, increasing CAPE while reducing CIN through warm-air advection aloft. Therefore, the increase of the CAPE and decrease of the CIN in the area surrounding the wet anomaly will increase the precipitation.

These findings are consistent with Froidevaux et al. (2014), who showed that convection is frequently initiated over drier surfaces near wetland boundaries, driven by

the thermal contrast between both areas. Despite elevated CAPE over wet patches, they observed the suppression of convection over these areas due to increased CIN and reduced surface heating.

A second mechanism is the large-scale impact of enhanced atmospheric moisture supply from tropical floodplains, which can increase precipitation over regions far larger than the floodplains themselves through a positive soil moisture–precipitation feedback (Eltahir 1998; Zheng and Eltahir 1998; Small and Kurc 2003). This feedback operates via changes in land–atmosphere coupling associated with increased soil moisture. As described by Eltahir (1998), wetter soils reduce surface albedo and Bowen ratio, increasing net radiation and favoring latent over sensible heat fluxes, which lowers surface temperature and reduces planetary boundary layer (PBL) depth.

Over large regions where horizontal advection is weak, the increased surface turbulent fluxes enhance moist static energy (MSE), which is the total energy (geopotential, sensible and latent heat) in a layer of the atmosphere, within a shallower PBL. Because entrainment, radiative cooling, and convective downdrafts are weakly affected by soil moisture, the net effect is an increase in PBL MSE and its vertical gradient, creating more unstable conditions that enhance the probability of convective events over the region. Eltahir (1998).

Small and Kurc (2003) summarise the positive feedback between soil moisture and precipitation from the previous studies of Betts and Ball (1998); Eltahir (1998); Zheng and Eltahir (1998) by the following four-step mechanism: (1) the wet soils have a lower Bowen ratio, which means they have higher latent heat fluxes compared to the sensible heat fluxes, (2) the lower Bowen ratio reduces the Planetary Boundary Layer Height (PBLH) due to the lower buoyancy of air parcels, (3) the shallower PBL induces the Moist Static Energy (MSE) to be more concentrated because of the low entrainment across the top of the Boundary Layer, (4) the higher MSE in the PBL increases the convective precipitation.

The Pantanal, a vast tropical floodplain in a semi-arid region, is the focus of this study due to its potential strong influence on land-atmosphere interactions. This work aims to address three key questions: (1) How do the Pantanal floodplains impact land-atmosphere interactions? (2) What are their effects on precipitation? (3) Why should floodplains be represented in Earth System and Regional Climate Models to improve realism, for example over the Pantanal where they influence large-scale circulation such as the South American Low-Level Jet (Montini et al. 2019)?

In this paper, we present the model and methodology, including a description of the region of interest, the RegIPSL modelling framework, and the design of the simulations, along with the observational datasets used for evaluation in Section 2. Section 3 presents the results and is organised into three parts: the impact on precipitation, the impacts in the vicinity of the Pantanal, and broader regional changes. Finally, we discuss the implications of these findings in Section 4 and conclude by summarising the main outcomes and their relevance for understanding regional climate processes in Section 5.

2 Model and Methodology

2.1 Region of Interest

The Pantanal is one of the world's largest tropical floodplains, a very flat region (between 80 and 150 m.a.s.l of altitude) covering approximately 150,000 km^2 (Hamilton et al. 1996; Alho 2005; Gonçalves et al. 2011). It is located in Central South America, primarily in western Brazil, but also extends into Bolivia and Paraguay. It is a UNESCO World Heritage Site and a Ramsar Wetland of International Importance. The region is highly dependent on seasonal hydrological processes, which are influenced by rainfall patterns and riverine dynamics within the Upper Paraguay River Basin (see Figure 1).

The Pantanal hydrological cycle is a *"flood pulse system"* (Junk et al. 1989), with a hydrological cycle that is distinctly seasonal driven by rainfall, which occurs predominantly during the wet season (October to March) (Schrapffer 2022). Rainfall over the Upper Paraguay River Basin upstream of the Pantanal contributes significantly to surface runoff, feeding the major rivers and floodplains of the Pantanal (Bravo et al. 2012). Seasonal flooding is the defining hydrological feature of the Pantanal.

Water from upstream rivers, such as the Paraguay, Cuiabá, and Taquari, inundates this low-lying region due to the slow drainage compared to a relatively large inflow. This water from precipitation occurring upstream of the Pantanal lasts between 3 and 5 months to reach the outflow of the Pantanal (Hamilton et al. 1996; Padovani 2010; Gonçalves et al. 2011). These hydrological dynamics not only define the ecological cycles of the region, but could also have a potential influence on local and regional climate.

The evaluation of the impact of soil moisture on the land atmosphere coupling has received a strong interest over the La Plata Basin (LPB) which has been studied using climate models as well as satellite data (Ruscica et al. 2016, 2015, 2014; Sörensson and Menéndez 2011; Spennemann et al. 2017; Menéndez et al. 2019; Coronato et al. 2020; Carril et al. 2016).

The precipitation in the LPB is strongly related to the atmospheric moisture transport from the South American Low-Level Jet (SALLJ; Zanin and Satyamurty 2020; Martinez and Dominguez 2014; Su and Lettenmaier 2009). During the austral summer, precipitation is fed by the atmospheric moisture transport by the tropical Atlantic, the subtropical south-western Atlantic, the tropical North Atlantic and the recycling of precipitation over the Amazon and LPB (Zanin and Satyamurty 2020). In austral winter, the precipitation in the LPB is more related to the recycling of precipitation from the Southern Amazon and Upper Paraguay River Basin (Zanin and Satyamurty 2020). Therefore, the Pantanal is an important source of moisture for the LPB precipitation during the austral winter. This is confirmed by (Su and Lettenmaier 2009) who showed that the Pantanal is the only region of the LPB that has a high recycling of evapotranspiration into precipitation in the basin throughout the year.

Another key driver related to the SALLJ is the Chaco Low (Seluchi and Marengo 2000). It is a low-pressure system that forms over the Gran Chaco region of South America, primarily during the austral summer (DJF). It is driven by intense surface

heating and contributes to regional circulation patterns. The Chaco Low plays a critical role in influencing atmospheric moisture transport of SALLJ from the Amazon Basin toward the La Plata Basin and southeastern South America and precipitation in these regions (Salio et al. 2002; Ferrero and Villalba 2019; Menéndez et al. 2024).

Although the South American Low-Level Jet is typically located west of the Pantanal along the Andes foothills, its position and intensity vary, allowing the Pantanal to influence the jet during eastward shifts or intensified events (Zanin and Satyamurty 2020; Martins et al. 2013) therefore, the impact of the floodplains on the atmosphere and, in particular, on the PBL can affect the SALLJ by enhancing/reducing atmospheric moisture transport and / or by deflecting it. Moreover, the extra evapotranspiration related to the presence of floodplains brings extra moisture to the SALLJ (Zanin and Satyamurty 2020). This could potentially lead to an impact of the Pantanal on the area downstreams of the SALLJ.

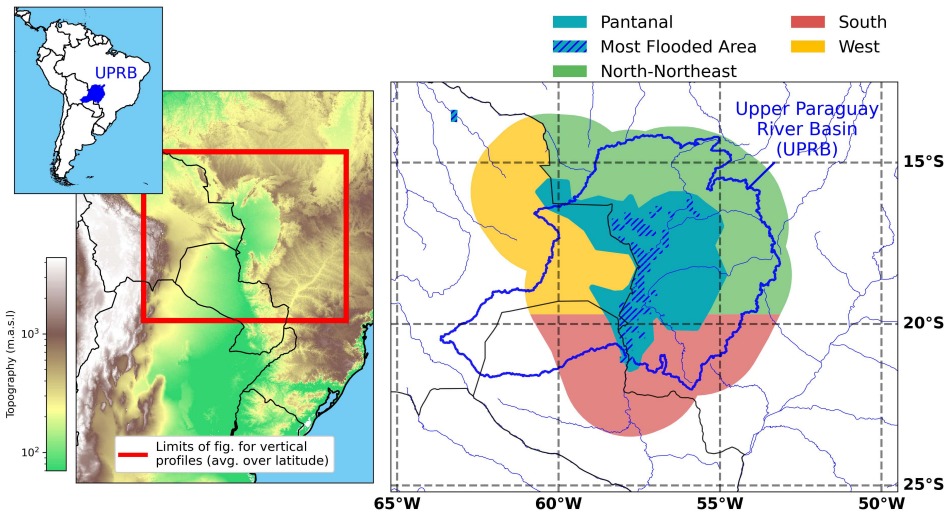


Fig. 1 Description of the Pantanal region, the Upper Paraguay River Basin and their location in South America. It also shows the most flooded area (F) and the limits are considered further for the latitudinal average. Additional regions used for further analysis are also detailed: South (S), West (W) and North-Northeast (NNE).

2.2 RegIPSL : Model description

The Regional Climate Model of the Institut Pierre Simon Laplace (IPSL), RegIPSL, follows the development of the MORCE-MED platform (Drobinski et al. 2012). RegIPSL couples 2 models representing different components of the Earth System: the Land Surface with the ORCHIDEE model (Organizing Carbon and Hydrology in Dynamic Ecosystems; Krinner et al. 2005) and the atmosphere with the WRF model

(Weather Research and Forecasting; Skamarock et al. 2008). These different models are coupled through the OASIS3-MCT coupler (Craig et al. 2017). The management of the Input and Output is performed by XIOS (XML-IO-Server), an asynchronous parallel I/O server. ORCHIDEE uses the same grid as WRF and the WRF-ORCHIDEE coupling follows the method from Polcher et al. (1998).

The WRF model is used in a large variety of climatological studies and for operational purposes within a large range of spatial and temporal scales (Powers et al. 2017). The version of WRF used in the RegIPSL simulations is version 3.7.1. The domain is a 20 km resolution Lambert Conformal projection covering the South American continent (cf. supplementary Figure S 2). The simulations considered 50 vertical levels with a top atmospheric pressure set at 10 hPa. The parameterisation is presented in Table 1. The deep and shallow convection is represented by the Grell-Devenyi ensemble cumulus scheme (Grell and Freitas 2014). A spectral nudging is used to avoid too large a deviation of the flow inside the domain from the prescribed boundary conditions, thereby improving the simulation's performance (Omrani et al. 2015). Only large-scale features above the PBL are nudged. This configuration is a standard configuration for the WRF model and has been selected after an extensive set of sensitivity test of the different WRF configurations in the ORCHIDEE-WRF coupled simulation over the domain.

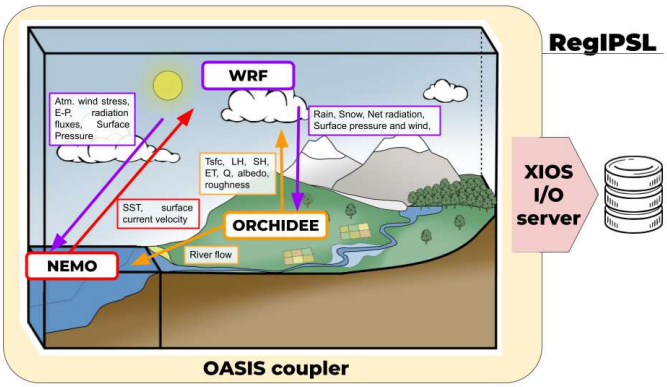


Fig. 2 Scheme of RegIPSL coupled model. In this work, NEMO model (Nucleus for European Modelling of the Ocean; Madec and the NEMO Team 2016) was not coupled to RegIPSL.

The ORCHIDEE model includes two main components : (1) SECHIBA, solving for the water and energy processes and fluxes, and (2) STOMATE for carbon processes and fluxes and for the vegetation dynamic. The soil hydrology is simulated through a 11-layer soil description (De Rosnay et al. 2000; de Rosnay et al. 2002; Campoy et al. 2013). The dynamical vegetation is simulated using 13 Plant Functional Types (PFTs) considered as a fraction of each grid cell, which all have different underlying parameters. Vegetation evolves, given a static definition of maximum PFT coverage per PFT type. The PFT description used in the simulation has been constructed from the ESA-CCI database (European Space Agency-Climate Change Initiative; ESA

Physics	Option	Reference
Microphysics	Morrison 2-moment scheme (M2M)	Morrison et al. (2009)
Planetary boundary layer	Mellor-Yamada-Nakanishi-Niino 2.5 scheme (MYNN)	Nakanishi and Niino (2009)
Radiation	Rapid Radiative Transfer Model for General Circulation (RRTMG)	Clough et al. (2005)
Deep and shallow convection	Grell-Freitas ensemble cumulus scheme	Grell and Freitas (2014)

Table 1 Parameterization of the WRF simulations.

2017). The river dynamic is simulated by the high-resolution river routing scheme based on the Hydrological Transfer Unit concept (Polcher et al. 2023) using the 2 km resolution version of MERIT-Hydro (Yamazaki et al. 2019)Numerical modelling of floodplains follows (Schrapffer et al. 2023). The maximal floodplains fraction over the HTUs is estimated using the interpolation of the GLWD dataset (WWF 2004) to the MERIT-Hydro grid (see supplementary Figure S **??**).

2.3 Simulations

Two simulations were performed over the period 1998-2019 with the exact same configuration except that one simulation includes the floodplains scheme (AmSud_Flood) and the other doesn't (AmSud_NoFlood). The lateral conditions are from ERA5 reanalysis Hersbach et al. (2020). The initial conditions of these simulations are based on a 10 years offline spin-up of the land surface variables and a 2-year spin-up of the atmospheric variables to ensure that the models are at equilibrium at the initialisation of the simulations.

2.4 Observations

The Global Precipitation Climatology Centre (GPCC) precipitation dataset (Schneider et al. 2017) is a gridded global precipitation pattern compiled and maintained by the Deutscher Wetterdienst (DWD). This dataset is constructed from in situ observations.

The monthly river discharge observations for the Porto Murtinho station (57.8911°W, 21.7003°S) are provided by the Brazilian National Hydrometeorological Network managed by the Brazilian National Water Agency (Agência Nacional de Águas – ANA).

Porto Murtinho is used as a reference outflow for the Pantanal (Schrapffer et al. 2023, 2020; Penatti et al. 2015).

3 Results

The results are structured hierarchically, beginning with the evaluation of the impact on precipitation over the region. This approach allows a clear identification of the broader impacts before delving into the underlying mechanisms. Following this initial assessment, the analysis is progressively refined across multiple spatial scales, such as the vicinity of the Pantanal and regional impacts.

3.1 Impact on Precipitation

Figures 3.a-d show the average seasonal precipitation for AmSud_Flood and provides on the main precipitation structure for the 4 seasons. The difference (Figure 3.e-h) is positive and significative over the Pantanal, its surrounding and extending west to the Pantanal toward the Andes and extending south down to the level of the south of the La Plata Basin. The increase in precipitation reaches values of up to 0.8 mm/d during the summer along the Andes and in the direct proximity of the Pantanal. Differences are smaller during the austral winter, but they are still significant due to the relatively low quantity of precipitation during this period, which corresponds to the dry season.

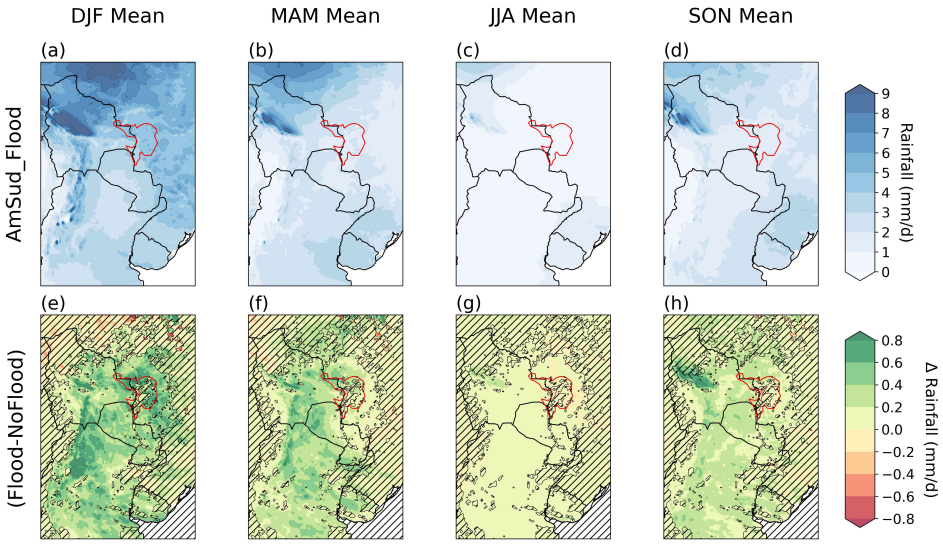


Fig. 3 Average precipitation for AmSud_Flood (a-d), and the difference between AmSud_Flood and AmSud_NoFlood between 1998 and 2019 (e-h). The average for the different seasons is shown: DJF (a,e), MAM (b,f), JJA (c,g) and SON (d,h). The differences of precipitation between AmSud_Flood and AmSud_NoFlood, which are not significant (significance level lower than 90% using a Student's t-test) are hatched in e-h.

Pantanal and its surroundings exhibit an increase in precipitation except some areas of the Pantanal. This spatial heterogeneity is linked to differences in land surface characteristics, which are further examined in Subsection 3.2, where we analyse the role of localised surface flux gradients and their influence on convection. The broader, regional-scale implications, including modifications in the atmospheric circulation and the possibility of remote effects, are presented in Subsection 3.3.

The differences in the diurnal cycle of precipitation during the wet season (DJF) between the AmSud_Flood and AmSud_NoFlood simulations are presented in Figure 4, referenced in local time (UTC-3). The period of major precipitation occurs during the afternoon (12:00–18:00), when AmSud_Flood shows a significant increase in precipitation across the Pantanal and its surrounding regions compared to AmSud_NoFlood. However, in the most heavily flooded areas, the difference in precipitation remains close to zero. During the evening (18:00–24:00), there is a notable increase in precipitation in AmSud_Flood compared to AmSud_NoFlood outside of the Pantanal, particularly in the northern and eastern regions. Additionally, smaller regions in the north-northwest and south-east of the Pantanal exhibit significant precipitation increases between 00:00 and 12:00.

Another feature of the simulations is the significant decrease and absence of increase in precipitation over the most flooded areas of the Pantanal in AmSud_Flood compared to AmSud_Flood, particularly during the evening hours and night (18:00–6:00). This suggests that the presence of floodplains alters the diurnal evolution of the PBL as flooded areas lead to a shallower and more stable PBL after sunset, which inhibits the development of moist convection during evening and night hours.

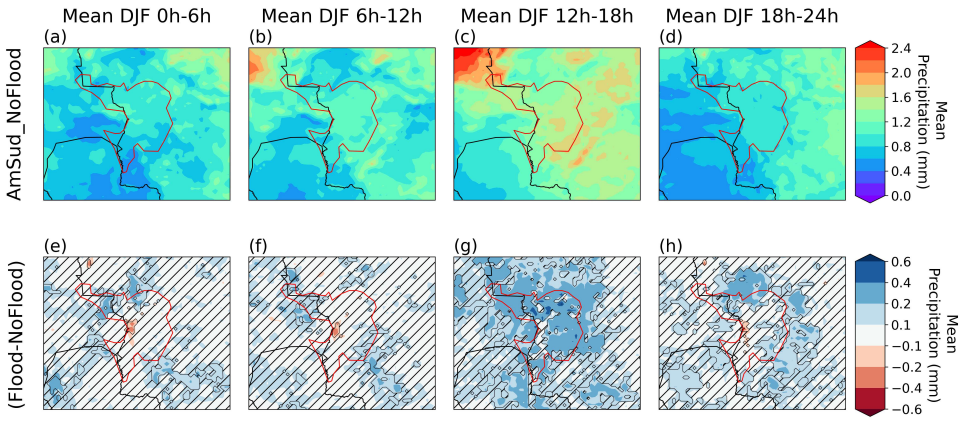


Fig. 4 Average diurnal cycle of precipitation for AmSud_NoFlood (a-d) and the difference between AmSud_Flood and AmSud_NoFlood (e-h) for the different 6-hour intervals of a day considered in the local time (UTC-3): 0h-6h (a,e), 6h-12h (b,f), 12h-18h (c,g) and 18h-24h (d,h) averaged between 1998 and 2019. The differences between AmSud_Flood and AmSud_NoFlood, which are not significant (significance level lower than 95% using a Student's t-test) are hatched.

To better understand the origin of precipitation differences between AmSud_Flood and AmSud_NoFlood, we examine whether these differences stem from a change in the frequency of rainfall events or from a change in their intensity.

Specifically two distinct factors are explored: (1) the number of rainless days (daily precipitation ¡ 1mm), and (2) the amount of precipitation recorded during those rainy days and the intensity of these events. A rainless day (rainy day) is defined as a day with precipitation lower (higher) than 1 mm.

Figure 5 shows the seasonal frequency of rainless days. Compared to GPCC observations, both simulations show a substantially higher number of rainless days, especially during DJF, MAM, and SON. Results are shown over the different regions: the Pantanal, North/East (NNE), South (S), West (W) and the most flooded area (F). See Figure 1.

Although comparing the simulations with observational datasets such as GPCC will provide further insight into potential model biases, the direct comparison between AmSud_Flood and AmSud_NoFlood simulations is already valuable for identifying the impacts of floodplain process integration on rainfall characteristics.

When comparing AmSud_Flood to AmSud_NoFlood, AmSud_NoFlood exhibits a higher ratio of rainless days during DJF, MAM, and SON across most regions, except in the most heavily flooded areas (F), where the opposite trend occurs. This suggests that floodplain dynamics contribute to reducing the number of rainless days in the AmSud_Flood simulation, particularly in wet season.

The total precipitation distribution for rainy days is similar in both simulations (see Figure S **??**). This indicates that the biases in total precipitation compared to GPCC between AmSud_Flood and AmSud_NoFlood are primarily due to differences in the number of rainy days rather than variations in daily rainfall intensity.

In summary, the analysis highlights that the key factor driving precipitation differences between the AmSud_Flood and AmSud_NoFlood simulations is the variation in the number of rainy days. This also represents the most significant divergence from GPCC observations. This is further discussed in Section 4.

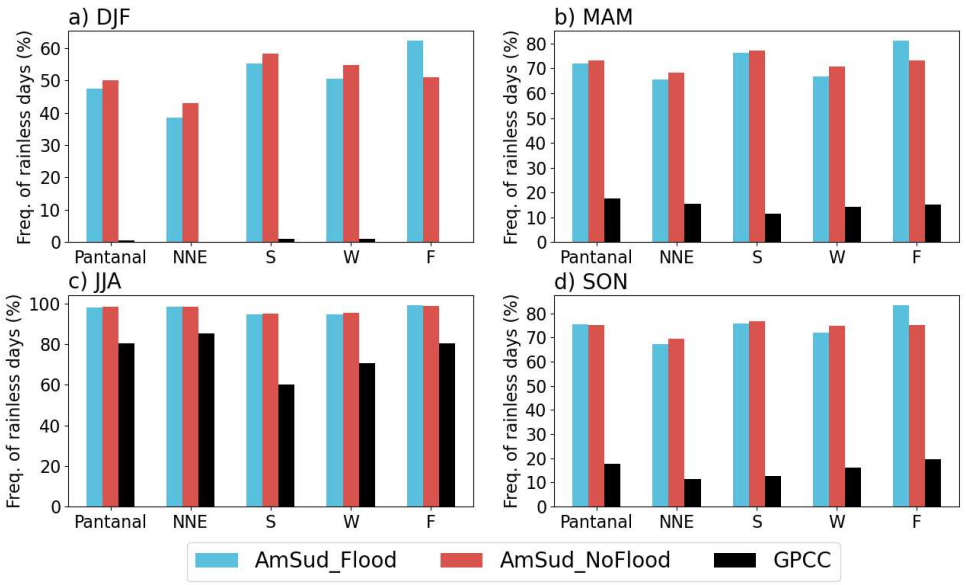


Fig. 5 Frequency of rainless days (PP<1mm) over the different regions: the Pantanal, North/East (NNE), South (S), West (W) and the most flooded area (F) between 1998 and 2019 for AmSud_Flood (in blue), AmSud_NoFlood (in red) and GPCC (in black) for the different seasons: DJF (a), MAM (b), JJA (c) and SON (d).

3.2 Impacts in the vicinity of the Pantanal

Figure 6 illustrates the annual cycle of various components of the hydrological cycle, including precipitation, discharge, evapotranspiration, and the sub-components of evapotranspiration over the Upper Paraguay River Basin (UPRB) and the Pantanal.

During the wet season, precipitation over the UPRB catchment is higher in the AmSud_Flood simulation compared to AmSud_NoFlood (Figure 6.a). However, when compared to observations (GPCC), the mean monthly precipitation is underestimated by about 2 mm/day during the wet season and by 0.4 mm/day during the dry season. The temporal dynamics of discharge at the UPRB outflow (Porto Murtinho) are better represented in AmSud_Flood than in AmSud_NoFlood, though discharge remains underestimated relative to observations (Figure 6.d) because of the underestimation of precipitation simulated over the basin.

Simulation with floodplains activated exhibits higher total evapotranspiration and transpiration throughout the whole year than AmSud_NoFlood (Figures 6.a and 6.c). The higher evaporation over the Pantanal in the floodplains simulation is directly associated with evaporation from flooded areas (Figure 6.e), a process absent in the AmSud_NoFlood simulation.

Interception, which represents the evaporation of water retained on vegetation surfaces, depends on the state of vegetation and precipitation. Although differences

in interception between simulations are minor (Figure 6.f), AmSud_Flood shows higher interception losses over the Pantanal during austral summer, which corresponds to increased precipitation and increased vegetation coverage, as already shown in Schrapffer et al. (2023).

Regarding bare soil evaporation over the Pantanal (Figure 6.b), it is higher in AmSud_NoFlood than in AmSud_Flood. This can be attributed to more bare soil in NoFlood as the vegetation cannot develop because of the lack of atmospheric moisture convergence.

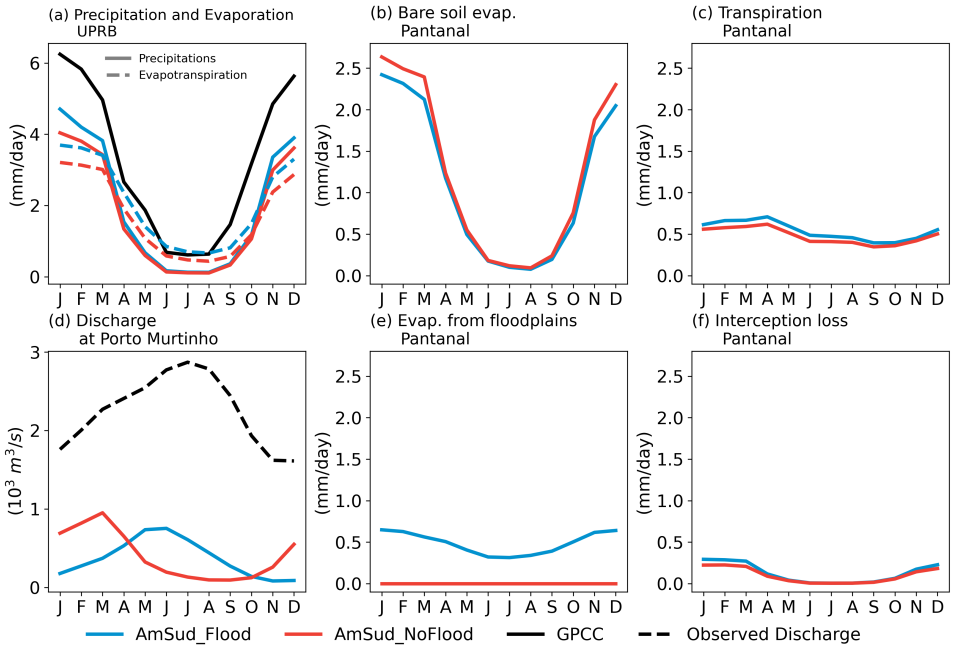


Fig. 6 Annual cycle for the 1998-2019 period (a) precipitation and evapotranspiration over the UPRB and (d) river discharge at Porto Murtinho as well as the annual cycle of the evapotranspiration components (b) bare soil evaporation, (c) transpiration, (e) evaporation from floodplains, (f) interception over the Pantanal in the AmSud_Flood (blue) and AmSud_NoFlood (red) simulation.

To better understand the hydrological balance, the analysis of precipitation changes is complemented by examining the precipitation minus evaporation (P-E) fluxes shown in Figure 7. P-E represents the net atmospheric contribution of water to the land surface. Positive P-E values indicate that precipitation exceeds evaporation, leading to soil moisture accumulation or potential runoff. In contrast, negative P-E values reflect a net loss of water to the atmosphere through evapotranspiration. Thus, P–E serves as a diagnostic for assessing whether a region acts as an atmospheric moisture sink or source over a given period, evaluating atmospheric moisture convergence.

Without floodplains activated, in the Amsud_NoFlood simulation, P-E is positive during the wet season (DJF) indicating a net gain of water at the surface. It has values close to zero during the onset of the wet season (SON). During the dry seasons (MAM and JJA), P-E becomes negative, revealing a soil moisture loss as evaporation exceeds the limited precipitation input. The soil moisture convergence at the surface does not compensate for the increased evaporation due to the activation of the floodplains. This seasonal pattern highlights the sensitivity of surface moisture availability to the rainfall annual cycle when floodplain processes are excluded.

In the AmSud_Flood simulation, the Pantanal flooded areas exhibit strong negative P-E values consistently (a difference of less than -0.8 mm/day with AmSud_NoFlood) throughout the year. This pattern contrasts significantly with the AmSud_NoFlood simulation, where P-E values are only positive during DJF. These lower P-E values over the most flooded areas are related to the evapotranspiration increase in AmSud_Flood compared to AmSud_NoFlood which is primarily driven by higher water availability due to increased precipitation during the preceding seasons (SON and DJF), which outweighs the relatively smaller precipitation increase in MAM and JJA.

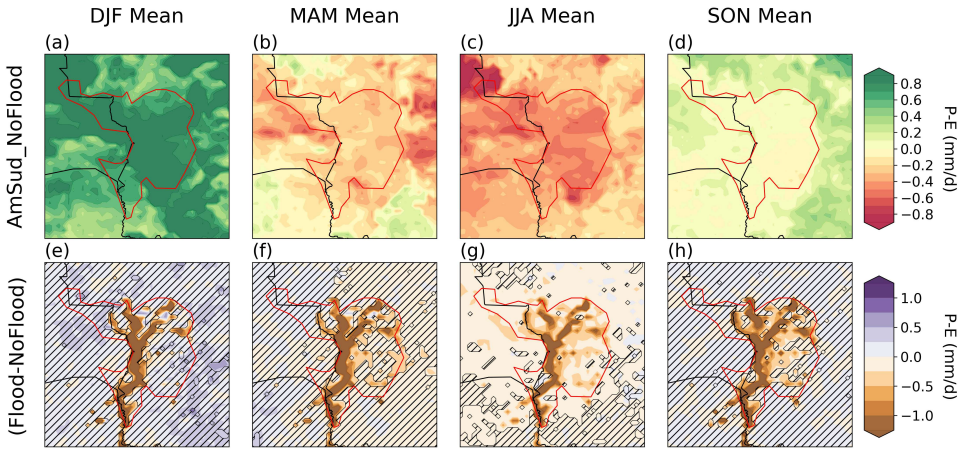


Fig. 7 Mean value of Precipitation minus Evapotranspiration for AmSud_NoFlood (a-d), and the difference between AmSud_Flood and AmSud_NoFlood (e-h) average over the different seasons : DFJ (a,e), MAM (b,f), JJA (c,g), SON (d,h). The differences between AmSud_Flood and AmSud_NoFlood, which are not significant (significance level lower than 95% using a Student's t-test) are hatched.

The MSE (Moist Static Energy) discussed in the introduction can be analysed through θ_e (equivalent potential temperature). Figure 8 illustrates the vertical profile of θ_e along the longitudinal axis of the Pantanal, averaged between 25°S and 12.5°S (see Figure 1). During DJF, there is a notable increase in θ_e at the surface and in the lower atmosphere and a decrease in the middle atmosphere across the entire longitudinal extent of the Pantanal in AmSud_Flood compared to AmSud_NoFlood (Figure 8.e). The low-level increase in θ_e reflects enhanced surface moisture and latent heat flux

associated with floodplain inundation. In JJA, the decrease at 700 hPa diminishes and becomes insignificant. There is a maximum instability in DJF over the entire transect.

The longitudinal profile of surface θ_e differences (Figure 8.i-l) aligns well with observed precipitation changes west of 60°W in DJF, MAM, and SON, and east of 56°W in DJF and SON. However, around the most flooded longitudes (approximately 57–58°W), θ_e increases while precipitation decreases. During JJA, the θ_e changes don't have a particular impact on the precipitation because the atmosphere is dry.

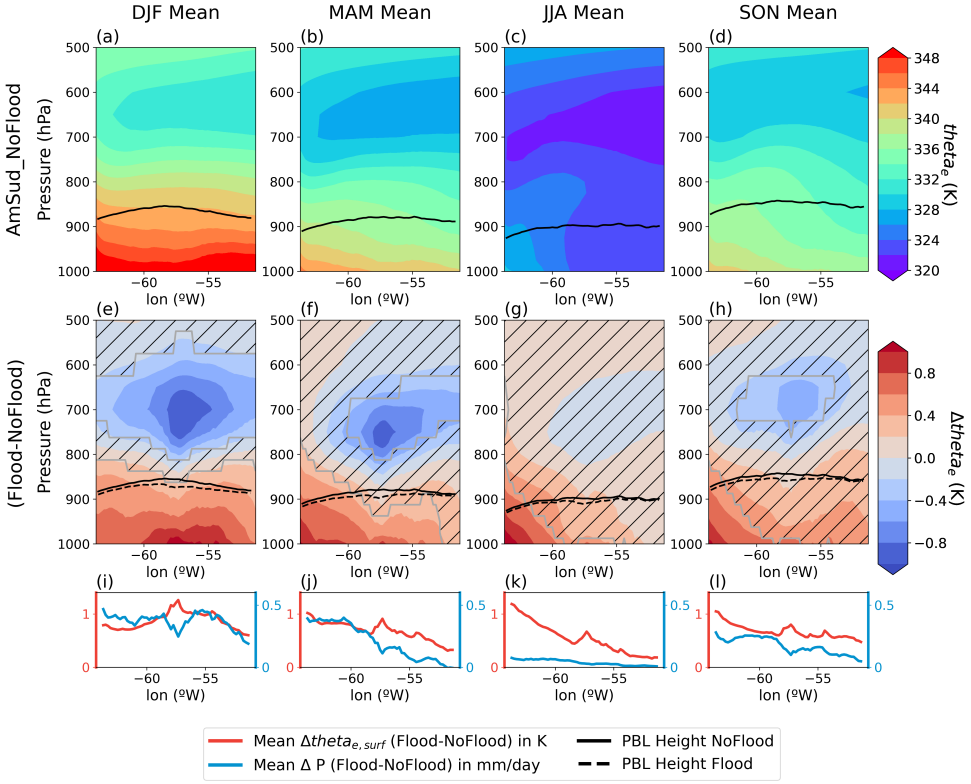


Fig. 8 Mean vertical profile of equivalent potential temperature between 25°S and 12.5°S for AmSud_NoFlood (a-d) and the relative difference between AmSud_Flood and AmSud_NoFlood (e-h) for the different seasons: DJF (a,e), MAM (b,f), JJA (c,g) and SON (d,h). The differences between AmSud_Flood and AmSud_NoFlood, which are not signitifant (significance level lower than 95% using a Student's t-test) are hatched. The average of the difference of near-surface equivalent potential temperature at 1000 hPa (in red) and precipitation (in blue) between AmSud_Flood and AmSud_NoFlood between 25o S and 12.5o S is shown for DJF (i), MAM (j), JJA (k) and SON (l).The planetary boundary layer height (PBLH) is shown in a-h with a black line, solid for AmSud_NoFlood simulation and dashed for AmSud_Flood simulation.

Figure 9 illustrates the mean vertical profile of specific humidity, averaged over the same latitude band, and highlights the contrasting effects of the floodplain scheme on atmospheric moisture. In general, in AmSud_Flood compared to AmSud_NoFlood, the specific humidity is higher over the low-level of the atmosphere (between 1000 hPa and 800 hPa) and is lower over the mid-level of the atmosphere (between 800 and 400 hPa) and it has higher values over the higher level (between 400 hPa and 200 hPa) which is an indicator of a less active PBL.

In the lower troposphere (1000–800 hPa), specific humidity is consistently higher in AmSud_Flood throughout the year. This increase is particularly significant during the dry season (JJA) and the early transition to SON, with increases reaching up to 8% in the western Pantanal during SON. This enhancement is directly linked to increased evapotranspiration from the floodplains, which amplifies its influence on atmospheric moisture during the drier parts of the year.

In contrast, the middle troposphere (800–400 hPa) exhibits a decrease in specific humidity in AmSud_Flood, with significant reductions occurring primarily during the wetter seasons of DJF and MAM. At these levels, drier free-tropospheric air replaces the moist air, leading to reduced specific humidity.

In the upper troposphere (400–200 hPa), specific humidity is higher in AmSud_Flood, though the increase is significant only during DJF and MAM. The changes in this layer, while less pronounced, suggest that floodplain-induced modifications to atmospheric moisture fluxes and convection also influence the upper tropospheric humidity.

The longitudinal profile of specific humidity changes in AmSud_Flood closely aligns with the longitudinal profile of evapotranspiration (Figure 9.i-l), showing a relation between surface processes and atmospheric moisture. This relationship confirms that the increase in specific humidity in the lower troposphere is directly driven by enhanced evapotranspiration over the floodplains.

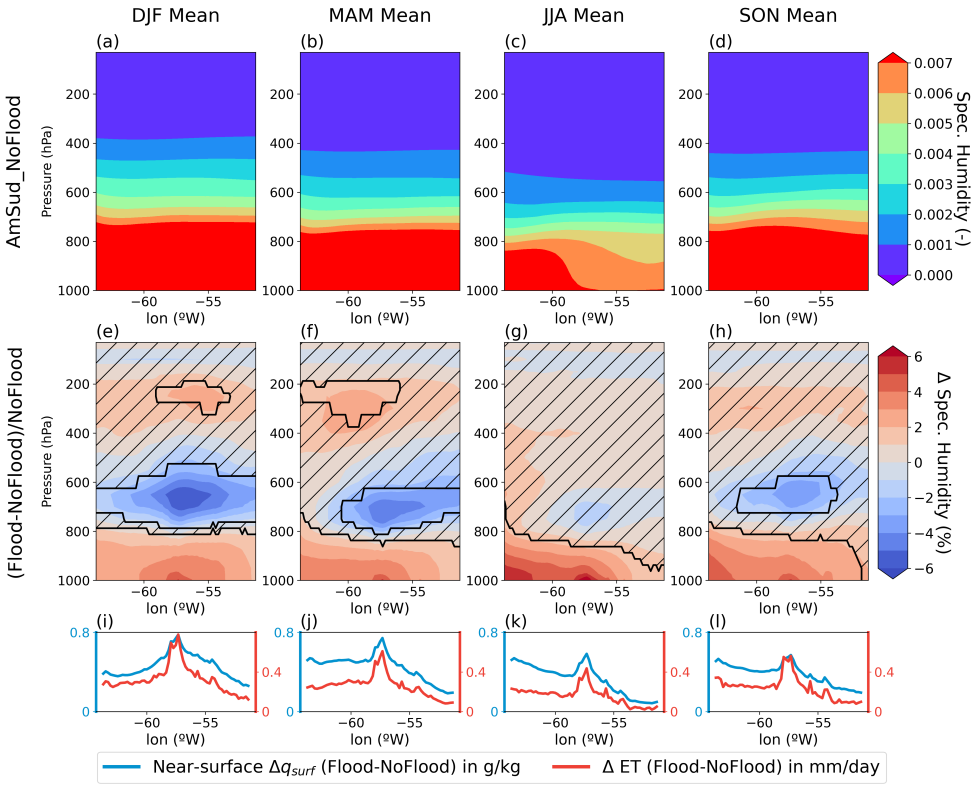


Fig. 9 Mean vertical profile of specific humidity between 25o S and 12.5o S for AmSud_NoFlood (a-d) and the relative difference between AmSud_Flood and AmSud_NoFlood (e-h) for the different season: DJF (a,e), MAM (b,f), JJA (c,g) and SON (d,h). The differences between AmSud_Flood and AmSud_NoFlood, which are not significant (significance level lower than 95% using a Student's t-test) are hatched. The average of the difference in near-surface specific humidity (in blue) and evapotranspiration (in red) between AmSud_Flood and AmSud_NoFlood between 25o S and 12.5o S is shown for DJF (i), MAM (j), JJA (k) and SON (l).

3.3 Regional Impacts

The analysis of the transport of atmospheric moisture allows to understand the larger scale influence of floodplains. Figure 10 illustrates the vertically integrated moisture transport (VIMT) from the surface to 500 hPa, following the methodology of Montini et al. (2019) to study the South American Low-Level Jet (SALLJ). Panels i to l of Figure 10 also show precipitation differences between the AmSud_Flood and AmSud_NoFlood simulations as colour shading.

The activation of the floodplain scheme weakens atmospheric moisture transport over the Pantanal and western adjacent areas in SON and DJF. The regions with the largest changes in moisture transport align well with wind changes (see Figure S **??**),

suggesting that the reduced transport be primarily due to weaker winds rather than a reduction in atmospheric humidity.

The atmospheric moisture transport increases west of the Pantanal along from Central Bolivia to central North Argentina throughout the year. This enhanced transport contributes to an increase in precipitation in these regions.

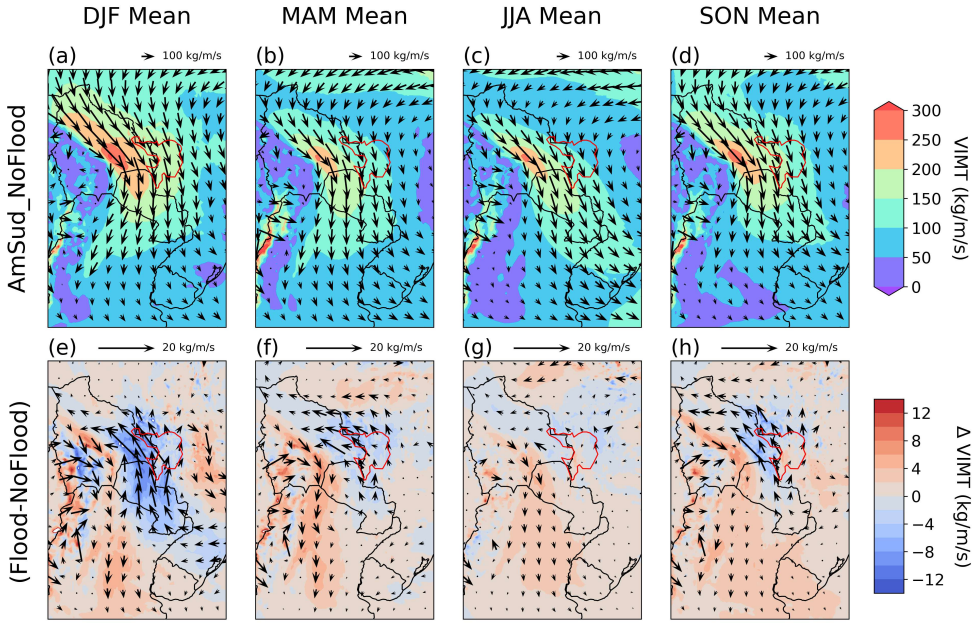


Fig. 10 Vertically integrated moisture transport from the surface to 500 hPa for AmSud_NoFlood (a-d) and the difference between AmSud_Flood and AmSud_NoFlood both between 1998 and 2019. The average for the different season is shown: DJF (a,e), MAM (b,f), JJA (c,g) and SON (d,h). The color panel on the subplots indicates the absolute value of the flux the AmSud_NoFlood (a-d) and the difference of the norm of the flux between AmSud_Flood and AmSud_NoFlood in (e,h). The direction of the flux is shown with black arrows.

The Hovmöller diagram (Hovmöller 1949) in Figure 11 presents the temporal anomalies of surface pressure compared to the average of the period between September and February (panels a-c) and surface temperature (panels d-f) for AmSud_NoFlood, AmSud_Flood, and their differences averaged over longitudes 65°W to 55°W from September to February during the 1998–2019 period. The pressure anomalies reveal a strong negative anomaly during DJF (December-February) between latitudes -35° and -20°, consistent with the typical location of the Chaco Low.

The difference between AmSud_Flood and AmSud_NoFlood simulations shows a positive anomaly in DJF compared to the overall average of the period between September and February, indicating a weaker Chaco Low in the AmSud_Flood simulation.

The surface temperature increases during the DJF period in Northeast Argentina (Figure 11.d), which lead to the development of the Chaco Low (Figure 11.a). When floodplains are considered, the additional precipitation cools the region, which might explain the lower temperatures compared to the AmSud_NoFlood simulation. Additional processes may also be involved, including (1) modifications of the surface radiative balance driven by changes in cloud cover, atmospheric humidity, and/or surface albedo, and (2) variations in evaporative demand, because a more humid atmosphere reduces evaporative losses and favors higher soil moisture. These lower temperatures in AmSud_Flood compared to AmSud_NoFlood are related to a decrease the Chaco Low intensity as observed through the higher geopotential in AmSud_Flood compared to AmSud_NoFlood.

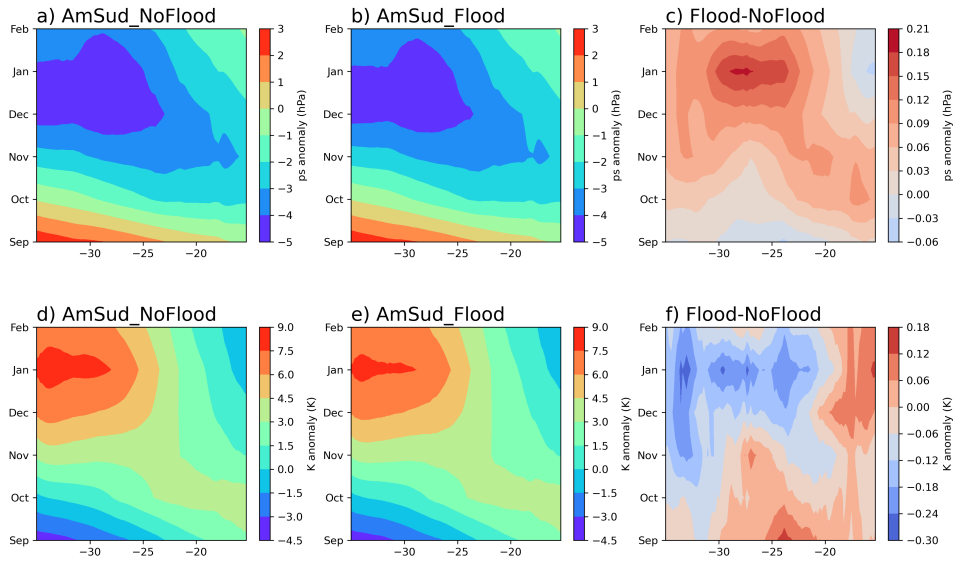


Fig. 11 Hovmöller diagram of the anomaly of surface pressure (a,b,c) and surface temperature (d,e,f) forAmSud_NoFlood (a,d), AmSud_Flood (b,e) and the difference between both (c,f) averaged over the longitude 65°W and 55°W from September to February considering the period 1998-2019 compared to the average of the period between September and February.

4 Discussion

The impact on precipitation described in Subsection 3.1 results align with the mechanisms described by both Adler et al. (2011) and Eltahir (1998). During the afternoon and evening, the planetary boundary layer (PBL) experiences peak Moist Static Energy (MSE) levels due to evapotranspiration from the floodplains throughout the day. This enhances the likelihood of convective precipitation. It is worth highlighting

that Adler et al. (2011) focuses on the localised precipitation changes over a moist band and its immediate drier surroundings, while Eltahir (1998) explains the broader processes responsible for increased precipitation across larger regions influenced by floodplain dynamics. The behaviour over the most flooded areas in central Pantanal along the Paraguay River is a separate process that has already been explained previously.

Concerning the precipitation bias displayed by the simulations seems to be a systematic issue of WRF, similar biases have been observed in different studies, such as Liu et al. (2025) in which a 4-km convection-permitting WRF simulation showed a few wet days but with larger precipitation intensity can be observed. This study also evaluated coarser resolution (12-km and 24-km simulations) simulations and observed that they greatly underestimate tropical rainfall. Gomes et al. (2022) also noticed systematic errors and areas with large uncertainties in precipitation with particular negative biases in some configurations over the South American continent based on regional climate simulations with WRF model.

The comparison was performed using GPCC data. However, it is important to note that the region contains only a limited amount of rain gauge stations, which may reduce the reliability and spatial representativeness of the GPCC product.

The increase soil moisture caused by the floodplains allows for high evapotranspiration, leading to negative P-E values and turning the region into a net source of atmospheric moisture.

Activating the floodplains scheme transforms the most flooded areas of the Pantanal from an atmospheric moisture sink (annual average $P - E > 0$) into a moisture source (annual average $P - E < 0$) due to the soil moisture convergence over land caused by the floodplains leading to higher evapotranspiration. This shift occurs because the scheme enables the evaporation of water transported to the region via the hydrological network, which is believed to be realistic and similar to what occurs over other tropical floodplains (Niger, Taylor et al. 2018; Sudd, Sutcliffe and Brown 2018). In tropical regions, where energy for evaporation is abundant but water availability limits moisture fluxes, this mechanism plays a critical role in maintaining atmospheric humidity.

The increase of θ_e with a decrease in precipitation in Figure 8 can be attributed to processes described by Adler et al. (2011): the surroundings of the Paraguay River, forming a moist band due to extensive flooding, lead to increased precipitation. However, the local dry/wet contrast causes a reduction in precipitation due to the fact that wet soils tend to have lower Bowen ratio and, therefore, a less turbulent PBL. This leads to cooler surface temperatures and lower PBLH, which suppresses precipitation, explaining the observed decline in precipitation at these longitudes despite an increase θ_e.

The comparative analysis of the simulations shows that the integration of the floodplains turned the Pantanal into an atmospheric moisture source that supplies humidity to the atmosphere in the regions downstream the SALLJ, increasing the regional precipitation.

At the larger scale, our results over the larger scale of the La Plata Basin, are coherent with Eltahir (1998) as we have lower Bowen ratio, a lower Planetary Boundary Layer, a higher Moist Static Energy in the Planetary Boundary Layer and an increased gradient of Moist Static Energy between the Planetary Boundary Layer and the mid-troposphere, which facilitates the convection in the region.

Larger scale impact affect regional climate featuressuch as the Chaco Low which is weakened by the increased atmospheric transport of moisture from tropical to subtropical South America (Ferrero and Villalba 2019) due to the activation of the floodplains in AmSud_Flood.

5 Conclusion

AmSud_Flood indicates that the Pantanal floodplains are an important atmospheric moisture source for the region and affect a certain number of atmospheric processes.

The activation of the floodplains scheme in the coupled simulations has an impact on precipitation through different mechanisms involved on different spatial scales. The impact of the floodplains on precipitation over the Pantanal confirms the observations from Taylor (2010) and Taylor et al. (2018) because the increase in rainfall during the wet season is mostly related to the afternoon precipitation and there is a decrease of precipitation over the most flooded parts of the Pantanal. This decrease is consistent with the mechanism described by Adler et al. (2011) because the local wetland breeze locally inhibits convection. The negative bias of precipitation over the most flooded areas in AmSud_Flood is related to an increase in rainless days, while the increase in precipitation over the rest of the Pantanal is related to an increase in rainy days.

On a larger scale, the activation of the floodplains scheme converts the Pantanal into an atmospheric source of moisture for the atmosphere, with a negative average $P-E$ flux over the most flooded areas, increasing the specific humidity, precipitation, soil moisture, and reducing the temperature in the lower atmosphere and decreasing the height of the PBL. Although there is no significant reduction in the middle troposphere temperature, there is a significant decrease in the specific humidity. This leads to higher equivalent potential temperatures in the low troposphere and lower over the middle troposphere. The presence of the Pantanal increases regional precipitation and impacts the land-atmosphere interactions through positive feedback between soil moisture and precipitation. These processes are probably specific to South America as this type of impact depends on the regional circulation.

The regional circulation is marked by the South American Low-Level Jet that brings moisture from the Amazon and the Upper Paraguay River Basin to the subtropical latitudes and is the principal source of humidity for the precipitation over the Gran Chaco. The presence of the floodplains affects the SALLJ by reducing the strength of the atmospheric moisture flux at the West of the Pantanal, principally through a wind speed reduction, while increasing the flux along the Eastern Andes. The mechanisms linking Pantanal flooding to changes in the South American Low-Level Jet (SALLJ) remain incompletely understood. However, based on our results, a physically consistent hypothesis can be proposed. In AmSud_Flood, the Chaco Low weakens, in agreement with the moisture flux anomalies. These anomalies feature northward flow east of the

Chaco Low—consistent with a weakened SALLJ—and southward flow to the west, which enhances moisture transport toward northwestern and central Argentina. This redistribution of moisture further weakens the Chaco Low, reinforcing the reduction in the SALLJ. The consistency between these circulation anomalies and the pressure patterns supports the hypothesis that Pantanal flooding influences the SALLJ indirectly through its impact on the Chaco Low.

The Pantanal shows how a large tropical floodplain in a semi-arid region affects the atmosphere locally and regionally through the regional circulation and, in particular, through a low-level jet feature. The Pantanal is a region that is very sensitive to local changes, such as vegetation changes related to wildfires, human activities affecting the land cover and river hydrology and regional precipitation changes. All these elements are threats to wetlands such as the Pantanal that may affect its hydrology and degrade its rich ecosystem.

Declarations

Funding This work was supported by Project PICT-2021-I-A-01097 funded by the Agencia Nacional de Promoción de la Investigación, el Desarrollo Tecnológico y la Innovación, and by Project PIP-112-2020-0102141-CO funded by the Consejo Nacional de Investigaciones Científicas y Técnicas (CONICET). Additional support was provided by the CLIMAT-AmSud program through Grant 21-CLI-MAT-01, Interaction between large-scale Atmospheric Circulation and dEforestation in the southern Amazon: implications for the local and continental water cycle (ACE-Amazon). This research also benefited from funding by CNRS INSU AO LEFE 2020 under the project PANTANAL: Impacts of tropical floodplains on the land–atmosphere interaction; the Pantanal case. Furthermore, this work was supported by the French–Argentine project ECOS-Sud 2018 (ECOS-A18D04), co-financed by the Ministerio de Ciencia, Tecnología e Innovación (MINCyT), Argentina, and Université Sorbonne Paris Nord, France.

Competing Interests The authors have no relevant financial or non-financial interests to disclose.

Data Availability The datasets generated during and/or analysed during the current study are not publicly available due to their large size and storage constraints, but are available from the corresponding author on reasonable request.

Author Contributions

Conceptualization and methodology were carried out by A.Sc., J.P., A.So., L.F., and C.M. Climate model simulations were performed by A.Sc., J.P., and L.F. Analysis and validation were conducted by A.Sc., J.P., A.So., L.F., and C.M. The original draft of the manuscript was written by A.Sc. All authors (A.Sc., J.P., A.So., L.F., and C.M.) contributed to reviewing and editing the manuscript.

References

Adler B, Kalthoff N, Gantner L (2011) The impact of soil moisture inhomogeneities on the modification of a mesoscale convective system: An idealised model study. Atmospheric Research https://doi.org/10.1016/j.atmosres.2011.03.013

Alho CJR (2005) The World's Largest Wetlands. The World's Largest Wetlands: Ecology and Conservation https://doi.org/10.1017/CBO9780511542091

Betts AK, Ball JH (1998) FIFE surface climate and site-average dataset 1987-89. Journal of the Atmospheric Sciences https://doi.org/10.1175/1520-0469(1998)055⟨1091:FSCASA⟩2.0.CO;2

Bonan GB (1995) Sensitivity of a GCM simulation to inclusion of inland water surfaces. Journal of Climate https://doi.org/10.1175/1520-0442(1995)008⟨2691:SOAGST⟩2.0.CO;2

Bravo JM, Allasia D, Paz AR, et al (2012) Coupled Hydrologic-Hydraulic Modeling of the Upper Paraguay River Basin. Journal of Hydrologic Engineering https://doi.org/10.1061/(ASCE)HE.1943-5584.0000494

Campoy A, Ducharne A, Cheruy F, et al (2013) Response of land surface fluxes and precipitation to different soil bottom hydrological conditions in a general circulation model. Journal of Geophysical Research Atmospheres https://doi.org/10.1002/jgrd.50627

Carril AF, Cavalcanti IF, Menéndez CG, et al (2016) Extreme events in the la Plata basin: A retrospective analysis of what we have learned during CLARIS-LPB project. Climate Research https://doi.org/10.3354/cr01374

Clough SA, Shephard MW, Mlawer EJ, et al (2005) Atmospheric radiative transfer modeling: A summary of the AER codes. Journal of Quantitative Spectroscopy and Radiative Transfer https://doi.org/10.1016/j.jqsrt.2004.05.058

Coronato T, Carril AF, Zaninelli PG, et al (2020) The impact of soil moisture–atmosphere coupling on daily maximum surface temperatures in Southeastern South America. Climate Dynamics https://doi.org/10.1007/s00382-020-05399-9

Craig A, Valcke S, Coquart L (2017) Development and performance of a new version of the OASIS coupler, OASIS3-MCT-3.0. Geoscientific Model Development https://doi.org/10.5194/gmd-10-3297-2017

De Rosnay P, Bruen M, Polcher J (2000) Sensitivity of surface fluxes to the number of layers in the soil model used in GCMs. Geophysical Research Letters https://doi.org/10.1029/2000GL011574

Dirmeyer PA (2011) The terrestrial segment of soil moisture-climate coupling. Geophysical Research Letters https://doi.org/10.1029/2011GL048268

Drobinski P, Anav A, Lebeaupin Brossier C, et al (2012) Model of the Regional Coupled Earth system (MORCE): Application to process and climate studies in vulnerable regions. Environmental Modelling and Software https://doi.org/10.1016/j.envsoft.2012.01.017

Eltahir EA (1998) A soil moisture-rainfall feedback mechanism 1. Theory and observations. Water Resources Research https://doi.org/10.1029/97WR03499

ESA (2017) Esa cci land cover time-series v2.0.7 (1992-2015). Tech. rep., European Space Agency-Climate Change Initiative

Ferrero ME, Villalba R (2019) Interannual and long-term precipitation variability along the subtropical mountains and adjacent chaco (22–29 s) in argentina. Frontiers in Earth Science 7:148

Finney DL, Marsham JH, Jackson LS, et al (2019) Implications of improved representation of convection for the East Africa water budget using a convection-permitting model. Journal of Climate https://doi.org/10.1175/JCLI-D-18-0387.1

Froidevaux P, Schlemmer L, Schmidli J, et al (2014) Influence of the background wind on the local soil moisture–precipitation feedback. Journal of the atmospheric sciences 71(2):782–799

Gomes HB, Lemos da Silva MC, Barbosa HdMJ, et al (2022) Wrf sensitivity for seasonal climate simulations of precipitation fields on the cordex south america domain. Atmosphere 13(1):107

Gonçalves H, Mercante M, Santos E (2011) Hydrological cycle. Brazilian Journal of Biology 71(1 suppl 1):241–253. https://doi.org/10.1590/S1519-69842011000200003

Grell GA, Freitas SR (2014) A scale and aerosol aware stochastic convective parameterization for weather and air quality modeling. Atmospheric Chemistry and Physics https://doi.org/10.5194/acp-14-5233-2014

Gula J, Richard Peltier W (2012) Dynamical downscaling over the Great Lakes Basin of North America using the WRF regional climate model: The impact of the great lakes system on regional greenhouse warming. Journal of Climate https://doi.org/10.1175/JCLI-D-11-00388.1

Hamilton SK, Sippel SJ, Melack J (1996) Inundation patterns in the Pantanal Wetland of South America determined from passive microwave remote sensing. Archiv für Hydrobiologie

Harding R, Blyth E, Tuinenburg O, et al (2013) Land atmosphere feedbacks and their role in the water resources of the ganges basin. Science of the Total Environment 468:S85–S92

Hersbach H, Bell B, Berrisford P, et al (2020) The era5 global reanalysis. Quarterly journal of the royal meteorological society 146(730):1999–2049

Hovmöller E (1949) The trough-and-ridge diagram. Tellus 1(2):62–66

Junk WJ, Bayley PB, Sparks RE (1989) The flood pulse concept in River-Floodplain Systems. In D P Dodge [ed] Proceedings of the International Large River Symposium Can Spec Publ Fish Aquat Sci 106:p. 110–127

Kohler M, Kalthoff N, Kottmeier C (2010) The impact of soil moisture modifications on CBL characteristics in West Africa: A case-study from the AMMA campaign. Quarterly Journal of the Royal Meteorological Society https://doi.org/10.1002/qj.430

Koster RD, Dirmeyer PA, Guo Z, et al (2004) Regions of strong coupling between soil moisture and precipitation. Science https://doi.org/10.1126/science.1100217

Koster RD, Chang Y, Wang H, et al (2016) Impacts of local soil moisture anomalies on the atmospheric circulation and on remote surface meteorological fields during boreal summer: A comprehensive analysis over North America. Journal of Climate https://doi.org/10.1175/JCLI-D-16-0192.1

Krinner G (2003) Impact of lakes and wetlands on boreal climate. Journal of Geophysical Research: Atmospheres https://doi.org/10.1029/2002jd002597

Krinner G, Viovy N, de Noblet-Ducoudré N, et al (2005) A dynamic global vegetation model for studies of the coupled atmosphere-biosphere system. Global biogeochemical cycles 19(1)

Kumar S, Newman M, Lawrence DM, et al (2020) The GLACE-Hydrology Experiment: Effects of Land-Atmosphere Coupling on Soil Moisture Variability and Predictability. Journal of Climate https://doi.org/10.1175/JCLI-D-19-0598.1

Liu C, Ikeda K, Prein A, et al (2025) Convection-permitting climate simulations over south america: Experimentation during different phases of enso. Atmospheric Research 316:107936

Lucas-Picher P, Laprise R, Winger K (2017) Evidence of added value in North American regional climate model hindcast simulations using ever-increasing horizontal resolutions. Climate Dynamics https://doi.org/10.1007/s00382-016-3227-z

Madec G, the NEMO Team (2016) NEMO ocean engine. Note du Pôle de modélisation

Martinez JA, Dominguez F (2014) Sources of Atmospheric Moisture for the La Plata River Basin*. Journal of Climate https://doi.org/10.1175/JCLI-D-14-00022.s1

Martins R, Sá L, Moraes O (2013) Low Level Jets in the Pantanal Wetland Nocturnal Boundary Layer – Case Studies. American Journal of Environmental Engineering https://doi.org/10.5923/j.ajee.20130301.06

Menéndez CG, Giles J, Ruscica R, et al (2019) Temperature variability and soil–atmosphere interaction in South America simulated by two regional climate

models. Climate Dynamics https://doi.org/10.1007/s00382-019-04668-6

Menéndez CG, Russmann JE, Giles JA, et al (2024) Influence of the cross-equatorial chaco-northwest africa pressure gradient on the south american monsoon. Climate Dynamics 62(11):10019–10032

Montini TL, Jones C, Carvalho LM (2019) The South American Low-Level Jet: A New Climatology, Variability, and Changes. Journal of Geophysical Research: Atmospheres https://doi.org/10.1029/2018JD029634

Morrison H, Thompson G, Tatarskii V (2009) Impact of cloud microphysics on the development of trailing stratiform precipitation in a simulated squall line: Comparison of one- and two-moment schemes. Monthly Weather Review https://doi.org/10.1175/2008MWR2556.1

Nakanishi M, Niino H (2009) Development of an improved turbulence closure model for the atmospheric boundary layer. Journal of the Meteorological Society of Japan https://doi.org/10.2151/jmsj.87.895

Notaro M, Bennington V, Vavrus S (2015) Dynamically downscaled projections of lake-effect snow in the Great Lakes basin. Journal of Climate https://doi.org/10.1175/JCLI-D-14-00467.1

Omrani H, Drobinski P, Dubos T (2015) Using nudging to improve global-regional dynamic consistency in limited-area climate modeling: What should we nudge? Climate Dynamics https://doi.org/10.1007/s00382-014-2453-5

Padovani (2010) Dinâmica Espaço-Temporal das Inundações do Pantanal. PhD thesis, Piracicaba: Escola Superior de Agricultura Luiz de Queiroz, Centro de Energia Nuclear na Agricultura, Universidade de São Paulo, URL http://www.teses.usp.br/teses/disponiveis/91/91131/tde-14022011-170515/pt-br.php

Paiva RC, Collischonn W, Tucci CE (2011) Large scale hydrologic and hydrodynamic modeling using limited data and a GIS based approach. Journal of Hydrology https://doi.org/10.1016/j.jhydrol.2011.06.007

Penatti NC, de Almeida TIR, Ferreira LG, et al (2015) Satellite-based hydrological dynamics of the world's largest continuous wetland. Remote Sensing of Environment https://doi.org/10.1016/j.rse.2015.08.031

Polcher J, McAvaney B, Viterbo P, et al (1998) A proposal for a general interface between land surface schemes and general circulation models. Global and Planetary Change https://doi.org/10.1016/S0921-8181(98)00052-6

Polcher J, Schrapffer A, Dupont E, et al (2023) Hydrological modelling on atmospheric grids: using graphs of sub-grid elements to transport energy and water. Geoscientific Model Development 16(9):2583–2606. https://doi.org/10.5194/gmd-16-2583-2023

Powers JG, Klemp JB, Skamarock WC, et al (2017) The weather research and forecasting model: Overview, system efforts, and future directions. Bulletin of the American Meteorological Society https://doi.org/10.1175/BAMS-D-15-00308.1

de Rosnay P, Polcher J, Bruen M, et al (2002) Impact of a physically based soil water flow and soil-plant interaction representation for modeling large-scale land surface processes. Journal of Geophysical Research: Atmospheres https://doi.org/10.1029/2001jd000634

Ruscica RC, Sörensson AA, Menéndez CG (2014) Hydrological links in Southeastern South America: soil moisture memory and coupling within a hot spot. International Journal of Climatology 34(14):3641–3653. https://doi.org/10.1002/JOC.3930

Ruscica RC, Sörensson AA, Menéndez CG (2015) Pathways between soil moisture and precipitation in southeastern South America. Atmospheric Science Letters https://doi.org/10.1002/asl2.552

Ruscica RC, Menéndez CG, Sörensson AA (2016) Land surface-atmosphere interaction in future South American climate using a multi-model ensemble. Atmospheric Science Letters https://doi.org/10.1002/asl.635

Salio P, Nicolini M, Saulo AC (2002) Chaco low-level jet events characterization during the austral summer season. Journal of Geophysical Research: Atmospheres 107(D24):ACL–32

Schneider U, Finger P, Meyer-Christoffer A, et al (2017) Evaluating the Hydrological Cycle over Land Using the Newly-Corrected Precipitation Climatology from the Global Precipitation Climatology Centre (GPCC). Atmosphere 8(12):52. https://doi.org/10.3390/atmos8030052

Schrapffer A (2022) High-resolution numerical analysis of land-river-floodplains-atmosphere interaction in la plata basin. Phd thesis, Institut Polytechnique de Paris and Universidad de Buenos Aires, URL https://theses.hal.science/tel-03683965v1, nNT: 2022IPPAX022, tel-03683965

Schrapffer A, Sörensson A, Polcher J, et al (2020) Benefits of representing floodplains in a Land Surface Model: Pantanal simulated with ORCHIDEE CMIP6 version. Climate Dynamics https://doi.org/10.1007/s00382-020-05324-0

Schrapffer A, Polcher J, Sörensson A, et al (2023) Introducing a new floodplain scheme in orchidee (version 7885): validation and evaluation over the pantanal wetlands. Geoscientific Model Development 16(20):5755–5782. https://doi.org/10.5194/gmd-16-5755-2023

Schubert SD, Suarez MJ, Pegion PJ, et al (2008) Potential predictability of long-term drought and pluvial conditions in the U.S. Great Plains. Journal of Climate https://doi.org/10.1175/2007JCLI1741.1

Seluchi ME, Marengo JA (2000) Tropical–midlatitude exchange of air masses during summer and winter in south america: Climatic aspects and examples of intense events. International Journal of Climatology: A Journal of the Royal Meteorological Society 20(10):1167–1190

Seneviratne SI, Wilhelm M, Stanelle T, et al (2013) Impact of soil moisture-climate feedbacks on CMIP5 projections: First results from the GLACE-CMIP5 experiment. Geophysical Research Letters https://doi.org/10.1002/grl.50956

Silva Dias MA, Silva Dias PL, Longo M, et al (2004) River breeze circulation in eastern Amazonia: Observations and modelling results. Theoretical and Applied Climatology https://doi.org/10.1007/s00704-004-0047-6

Skamarock WC, Klemp JB, Dudhia J, et al (2008) A description of the advanced research WRF version 3, NCAR Tech. Note, NCAR/TN-468+STR. Natl Cent for Atmos Res Boulder, Colorado

Small EE, Kurc SA (2003) Tight coupling between soil moisture and the surface radiation budget in semiarid environments: Implications for land-atmosphere interactions. Water Resources Research https://doi.org/10.1029/2002WR001297

Sörensson AA, Menéndez CG (2011) Summer soil-precipitation coupling in South America. Tellus, Series A: Dynamic Meteorology and Oceanography https://doi.org/10.1111/j.1600-0870.2010.00468.x

Spennemann PC, Rivera JA, Osman M, et al (2017) Assessment of seasonal soil moisture forecasts over Southern South America with emphasis on dry and wet events. Journal of Hydrometeorology https://doi.org/10.1175/JHM-D-17-0015.1

Su F, Lettenmaier DD (2009) Estimation of the surface water budget of the La Plata Basin. Journal of Hydrometeorology https://doi.org/10.1175/2009JHM1100.1

Sutcliffe J, Brown E (2018) Water losses from the sudd. Hydrological Sciences Journal 63(4):527–541

Taylor CM (2010) Feedbacks on convection from an African wetland. Geophysical Research Letters https://doi.org/10.1029/2009GL041652

Taylor CM, Prigent C, Dadson SJ (2018) Mesoscale rainfall patterns observed around wetlands in sub-Saharan Africa. Quarterly Journal of the Royal Meteorological Society https://doi.org/10.1002/qj.3311

Vanderkelen I, van Lipzig NPM, Sacks WJ, et al (2021) Simulating the Impact of Global Reservoir Expansion on the Present-Day Climate. Journal of Geophysical Research: Atmospheres 126(16):e2020JD034485. https://doi.org/10.1029/2020JD034485

Wright DM, Posselt DJ, Steiner AL (2013) Sensitivity of lake-effect snowfall to lake ice cover and temperature in the great lakes region. Monthly Weather Review https://doi.org/10.1175/MWR-D-12-00038.1

WWF (2004) Global Lakes and Wetlands Database GLWD. GLWD Documentation pp 1–7. URL http://www.worldwildlife.org/pages/global-lakes-and-wetlands-database

Yamazaki D, Ikeshima D, Sosa J, et al (2019) MERIT Hydro: A high-resolution global hydrography map based on latest topography datasets. Water Resources Research p 2019WR024873. https://doi.org/10.1029/2019WR024873

Zanin PR, Satyamurty P (2020) Hydrological processes interconnecting the two largest watersheds of South America from seasonal to intra-monthly time scales: A critical review. International Journal of Climatology https://doi.org/10.1002/joc.6443

Zheng X, Eltahir EA (1998) A soil moisture-rainfall feedback mechanism 2. Numerical experiments. Water Resources Research https://doi.org/10.1029/97WR03497

Supplementary Files

This is a list of supplementary files associated with this preprint. Click to download.

- SupplementaryMaterial.pdf